

Public-data File 85-7

A REFRACTION PROFILE FROM HATCHER PASS TO SEWARD, SOUTH-CENTRAL ALASKA

By

J.N. Davies

Alaska Division of
Geological and Geophysical Surveys

March 1985

THIS REPORT HAS NOT BEEN REVIEWED FOR
TECHNICAL CONTENT (EXCEPT AS NOTED IN
TEXT) OR FOR CONFORMITY TO THE
EDITORIAL STANDARDS OF DGGS.

794 University Avenue, Basement
Fairbanks, Alaska 99701

FINAL REPORT

to

THE DEPARTMENT OF TRANSPORTATION AND PUBLIC FACILITIES

for a project entitled

A REFRACTION PROFILE FROM HATCHER PASS TO SEWARD, SOUTH CENTRAL ALASKA

by

Dr. John N. Davies
State Seismologist
Alaska Division of Geological and Geophysical Surveys
and
Adjunct Associate Professor of Geophysics
Geophysical Institute
University of Alaska

March 1985

TABLE OF CONTENTS

	Page
EXECUTIVE SUMMARY.....	1
ABBREVIATIONS.....	2
BACKGROUND.....	2
INSTALLATION OF TEMPORARY STATIONS.....	3
DATA ANALYSIS AND INTERPRETATION.....	4
DISCUSSION.....	6
FUTURE WORK.....	7
CONCLUSIONS.....	8
ACKNOWLEDGEMENTS.....	9
TABLES.....	10
FIGURES.....	14

EXECUTIVE SUMMARY

Late in the fall of 1982 Alaskan seismologists became aware that large explosions were being detonated near Bird Creek on Turnagin Arm. These explosions were for the purpose of widening the Seward Highway south of Anchorage. The largest of these explosions, about 33,000 lbs of TNT, could be seen on records made by the seismograph at McKinley Station, some 300 km distant from the blast site. Also visible on the records of the many seismographs around the Susitna and Matanuska Valleys and the Kenai Peninsula were some distinct secondary arrivals. A careful analysis of these arrival times has given a good calibration of the velocities of the crustal layers beneath the Matanuska Valley and the Kenai Peninsula. These velocities are fundamental data required to more precisely locate earthquakes in the region.

By the time we learned of the blasts only two large ones remained; they were scheduled for October 19 and 26, 1982. A joint project was agreed upon by the following agencies:

1. U.S. Geological Survey, Menlo Park, CA
2. Geophysical Institute, University of Alaska, Fairbanks
3. Division of Geological and Geophysical Surveys, Fairbanks
4. Alaska Tsunami Warning Center, Palmer
5. Research Section, Division of Planning and Programs, DOT/PF,
Fairbanks

The USGS deployed stations along the Seward Highway south of the blast site. The DGGs and the Geophysical Institute deployed instruments to the north of the blast site. The Tsunami Warning Center provided logistic support, facilities and special recording of the stations deployed by UAGI and DGGs. The Research Section provided financial support to UAGI and liaison between the scientists in the field and the contractor at the blast site.

About 16 temporary stations were established, eight to the south and eight to the north of the blast site. Sharp and clear arrivals were recorded at about 10 of these stations as well as at several of the permanent stations. Preliminary results show that adjustments should be made to the velocity model for the Kenai Peninsula and Matanuska Valley.

The velocity model derived here shows an upper layer about 2 km thick with a P-wave velocity of 5.55 km/sec in comparison to the value currently in use of 2.75 km/sec; the second layer has a velocity of 6.22 km/sec beginning at 2 km depth and extending to 15-20 km depth. P-wave velocities used in other models for the area don't reach 6.2 km/sec at depths shallower than 10 km.

ABBREVIATIONS

The following abbreviations are used throughout the report:

ATWC	Alaska Tsunami Warning Center, NOAA
DOT/PF	Dept. of Transportation and Public Facilities, State of Alaska
UAGI	University of Alaska, Geophysical Institute
USGS	United States Geological Survey
DGGS	Division of Geological and Geophysical Surveys, State of Alaska.

BACKGROUND

During the late summer of 1982 personnel of the seismology groups at the USGS in Menlo Park and at the Geophysical Institute in Fairbanks became aware that some rather large blasts were being set off in connection with a DOT/PF project to improve the Seward Highway in the vicinity of Bird Creek, on Turnagain Arm (see Figure 1). Some of these blasts were large enough to be

recorded by regional seismograph stations at distances up to 300 km from Bird Creek. It was agreed that some useful information about the structure of the crust could be obtained by deploying some temporary seismograph stations along a generally north-south alignment from Hatcher Pass (HTP, Figure 1) to Seward. Further, a general division of responsibility was assigned whereby the USGS would install stations from Bird Creek south to Seward and would record shot times, and a UAGI/DGGS group would install stations from Bird Creek north to Hatcher Pass. Below, we report only on the northern part of the project carried out by UAGI and DGGS personnel with financial support from DOT/PF and assistance from personnel at the ATWC.

INSTALLATION OF TEMPORARY STATIONS

Eight temporary stations were installed north of Bird Creek. The locations of these stations are shown by the open triangles in Figure 1 and their coordinates and other information related to their locations are given in Table 1. These were all standard UAGI short-period, vertical-component telemetered seismic stations. They consisted of Geotech S-13, 1 Hz seismometers, Monitron amplifier-VCOs, and Monitron VHF transmitters.

Signals were recorded at the ATWC Observatory at Palmer. An unused USGS Develocorder (16 mm film recorder) was pressed into service along with some of their spare Develco discriminators. The radio frequency signals were picked up at Palmer using UAGI Monitron receivers. Film and record-changing were provided by ATWC.

The seismic signals from the eight temporary stations were recorded along with signals from nine permanent, regional stations operated respectively by the USGS, ATWC and UAGI. The locations of the regional stations are shown by the solid triangles in Figure 1 and their coordinates and other information

are given in Table 1. This combination of temporary and permanent stations was operated for 14 days from October 15, 1982 through October 28.

DATA ANALYSIS AND INTERPRETATION

Three blasts were recorded, one on October 19 and two on October 26. The origin times, locations and sizes of these three events (nos. 5, 6 and 7) and four other blasts are given in Table 2. The location of the blasts relative to the seismic stations is shown in Figure 1 (note that on the scale of this figure the individual locations of the blasts are indistinguishable). The film records of the blasts were scaled on a GeoTech film viewer just as if they had been earthquakes. The arrival times of distinctive phases were read to the nearest twentieth of a second. The arrival times were then corrected for the elevation of the station (above sea level) and converted to travel times from Bird Creek to the individual stations by subtracting the origin time:

$$TT = AT - C(E) - OT \quad (1)$$

where TT is the corrected travel time, AT is the raw arrival time, C(E) is the elevation correction ($E \div 5$ km/sec) and OT is the origin time of the blast. The C(E) are given in Table 1 for each station; the OT are given in Table 2 for each blast. The TT are summarized in Table 3 and are plotted against distance to the respective seismic station in Figure 2.

The simplest way to interpret these data is to fit them to a model of the crustal structure which consists of N horizontal layers. The travel time as a function of distance, D, for such a model is:

$$TT_1 = \frac{D}{V_{i+1}} + 2 \sum_{j=1}^i \frac{H_j \cos \theta_j}{V_j} \quad (2)$$

where TT_1 is the travel time for the wave refracted along the bottom of the i^{th} layer, D is the distance from shot to station, V_i is the P-wave velocity in the i^{th} layer, H_j is the thickness (km) of the j^{th} layer and θ_j^1 is the angle the ray path makes with the vertical in the i^{th} layer for the ray bottoming just below the j^{th} layer. Therefore, the slope of a straight line in Figure 2 is $\frac{1}{V_{i+1}}$, so the inverse of the slope of the i^{th} branch of the travel time curve is the velocity of the $(i+1)$ st layer. And the corresponding intercept of the i^{th} branch is:

$$I_i = 2 \sum_{j=1}^i \frac{H_j \cos \theta_j^1}{V_j} \quad (3)$$

which can be rewritten

$$H_j = \frac{V_i}{\cos \theta_i^1} \left[\frac{I_i}{2} - \sum_{j=1}^{i-1} \frac{H_j \cos \theta_j^1}{V_i} \right] \quad (4)$$

which can be solved iteratively for the layer thicknesses given the V_i and I_i from the various branches of the travel-time vs. distance plot such as is shown in Figure 2.

In the present case we assume only one layer over a half space so we have fit two branches to the data: one for the direct arrival which travels only in the top layer and a second one for the refracted ray path which follows the top of the half space.

In Figure 2 the line which goes through the origin and the open symbols corresponds to the direct arrival. The goodness-of-fit measure, r^2 , for this line is 0.998. The inverse of the slope of this line gives a velocity of 5.55 km/sec for the first layer. The line through the solid symbols corresponds to the refracted arrivals and has a goodness-of-fit measure of r^2

= 0.998. This line has an inverse slope of 6.22 km/sec and an intercept time of 0.30 sec. Using this intercept time and these two velocities (5.55 and 6.22) equation (4) gives 1.84 km for the thickness of the layer. Summarizing, we have a layer 1.84 km thick with a velocity of 5.55 km/sec which overlies a half space with a velocity of 6.22 km/sec.

To check this model we can use equation (2) to calculate the expected travel times for the refracted ray to each of the seismic stations in our experiment. Simplifying (2) we have:

$$TT_1 = \frac{D}{V_2} + 2 \frac{H_1 \cos \theta_1}{V_1} \quad (5)$$

where D is the distance to the station, $V_1 = 5.55$ km/sec, $V_2 = 6.22$ km/sec, $H_1 = 1.84$ km and $\theta_1 = 63.16$ degrees (from Snell's Law).

Using (5) the expected travel times, $\langle TT \rangle$, have been calculated and compared to the mean travel time, \overline{TT} for each station. This comparison is shown in Table 4. The standard deviation of the difference between the expected and observed travel times is 0.29 seconds, and the worst case is 0.61 seconds. Considering the simplicity of the model and the variety of geologic settings for the various seismic stations this is quite a good fit between model and data.

DISCUSSION

While this is a reasonably good fit to the majority of the better quality data (i.e., those where a particular travel time is seen at a station for two or three of the blasts), there are many arrivals which are not explained by this model, some of which are quite strong. In particular, note the 8.3 second travel time at 27.5 km (PMS). This was quite strong and seen at PMS for two of the blasts. If this arrival is interpreted as a reflection from the bottom of the 6.22 km/sec layer it would suggest that this layer is about 20 km thick.

During the past summer the USGS shot a detailed refraction line from near Valdez to Paxson. One of the more interesting features of this line is a series of "en echelon" sets of arrival times which suggests that the crust is composed of alternating layers of high and low velocity. A line fit to the more distant end of each of these sets has a slope which corresponds to a "velocity" of about 6.2 km/sec. These sets of arrivals are limited to stations grouped in 10-15 km intervals (the station spacing for the USGS line was about 1-2 km). This suggests that as a result of the sparse station spacing of the present experiment (about 10-20 km) the results may be spatially aliased so that there is in fact no thick layer with a velocity of 6.22 km/sec.

However, the crustal model obtained here is still quite useful for locating earthquakes using sparse networks of seismograph stations. Further, if the secondary arrivals which don't fall on the two main branches in Figure 2 (the simple error bars) do correspond to arrivals from a stack of high and low velocity layers, there is no obvious, unique, en echelon pattern to them. Therefore, the very simple model used here is probably the most appropriate one, given the nature of the data from the present experiment.

FUTURE WORK

With respect to the data collected during this experiment, there are four remaining tasks which would be useful to complete:

- (1) Incorporate the data from the USGS stations to the south of Bird Creek.

It may be worthwhile to digitize the UAGI data since the USGS data were digitally recorded. This would make possible a more uniform approach to processing the data.

- (2) Refine and extend the velocity model. This would include an iterative evaluation of the arrival time picks in light of the predicted arrival times from the model, in terms of both the times and the relative amplitudes of the various phases. It should be possible to read more reflected phases to constrain the depth of the base of the 6.22 km/sec layer. Consideration might be given to any evidence for dipping layers.
- (3) Read arrival times from other blasts at the regional stations of UAGI, ATWC and USGS. "Relocation" of the blasts as if they were earthquakes using the crustal model derived in step (2) might shed light on station corrections for routine use in the location of earthquakes in the greater Anchorage area.
- (4) Read arrival times from earthquakes in the Matanuska Valley during the period October 14-28 when the UAGI temporary stations were operational. Combining these stations with the permanent stations gives a relatively dense station coverage during this period. Earthquakes "caught" by this net might be quite accurately located and then used to calibrate station corrections for more distant stations as suggested for the blast data in (3) above.

CONCLUSIONS

A preliminary interpretation of arrival time data at stations to the north of the Bird Creek blasts suggests that the crustal velocities in the upper 15-20 km can be described by a simple two-layer model:

<u>Layer</u>	<u>Depth Range (km)</u>	<u>Velocity (km/sec)</u>
1	0-1.84	5.55
2	1.84-22(?)	6.22

This model "predicts" the first arrival at 16 stations ranging in distance from the blast from 11.94 km to 154.63 km with standard deviation of 0.29 seconds for the differences between observed and predicted arrival times.

ACKNOWLEDGEMENTS

This work was supported from a grant from the Department of Transportation and Public Facilities and by internal funds of the U.S. Geological Survey, the State Division of Geological and Geophysical Surveys, the Geophysical Institute and the Alaska Tsunami Warning Center. Scientific personnel -- John N. Davies, Larry Gedney, Steve Estes, Larry Kent, Dick Siegrist; Larry Sweet (Division of Research, DOTPF); Staff, Tsunami Warning Center, Palmer; Robert Page (USGS, Menlo Park, CA).

TABLE 1

CODE	NAME	LAT(N)	LONG(W)	ELEV(m)	DIST(km)	CORR(S)	OP'R	MAP
FTP	Flat Top	61.1082	149.2083	427	11.94	-0.09	UA-T	A-8
PMS	Arctic Valley	61.2447	149.5606	716	27.38	-0.14	ATWC	
PRC	Peters Creek	61.3902	149.4503	198	44.47	-0.04	UA-T	B-7
EKR	Eklutna Res.	61.4305	149.2583	427	53.36	-0.09	UA-T	B-6
SBY	Settlers Bay	61.5155	149.6238	76	56.91	-0.02	UA-T	C-7
RPZ	Rapunzel	61.4860	149.1102	76	61.26	-0.02	UA-T	B-6
PMR	Palmer Obs.	61.5922	149.1309	100	71.33	-0.02	ATWC	
PWA	Houston	61.6508	149.8787	137	72.78	-0.03	ATWC	
SSN	Susitna	61.4638	150.7433	1297	77.00	-0.26	USGS	
PME	Palmer East	61.6283	149.0211	232	77.06	-0.05	ATWC	
KNK	Knik	61.4125	148.4557	595	79.07	-0.12	USGS	
RIZ	Risley	61.7090	149.2233	290	81.81	-0.06	UA-T	C-6
MUR	Murdock	61.7710	149.8035	335	85.55	-0.07	UA-T	D-8
HTP	Hatcher Pass	61.7777	149.2767	917	88.43	-0.18	UA-T	D-7
SAW	Sawmill	61.8082	148.3330	740	114.02	-0.15	USGS	
SKN	Skwenta	61.9803	151.5297	564	146.69	-0.11	USGS	
SCM	Sheep Mtn.	61.8333	147.3277	1020	154.63	-0.20	UA	

Distance = vector difference in position between station and shot point.

Correction = travel from zero-elevation datum to station at 5 km/s

Operator: ATWC = Alaska Tsunami Warning Center
 UA = University of Alaska
 UA-T = University of Alaska, temporary station
 USGS = United States Geological Survey

Map: for UA-T stations gives Anchorage 1:63,000 quadrangle designation

TABLE 2

1982 Bird Creek Blasts: Origin Time, Location and Size

#	Date	Time* (GMT)		Location		Size KLB
		HR MN	SEC	N. Long.	W. Lat.	
1	SEP 21 (SEP 20)	0417 1917)	23.54 ± .04	-	-	18.4
2	SEP 23 (SEP 22)	0413 1913)	29.37 ± .04	61° 00.30'	149° 40.40'	21.4
3	OCT 05 (OCT 05)	1902 1002)	30.37 ± .02	-	-	19.7
4	OCT 12 (OCT 12)	1845 0945)	07.90 ± .01	- -	-	11.3
5	OCT 19 (OCT 19)	2233 1333)	03.13 ± .01	61° 00.20'	149° 39.95'	22.7
6	OCT 26 (OCT 26)	1846 0946)	10.85 ± .02	61° 00.20'	149° 40.10'	6.95
7	OCT 26 (OCT 26)	1912 1012)	23.53 ± .01	61° 00.20'	149° 39.65'	-

*Local time is given in parentheses.

TABLE 3

Explosion #	Station	Distance (km)	Corrected Travel Times						
			1	2	3	4	5	6	7
5	FTP	11.94			2.58				
6			2.18	2.36			5.26		
7			2.18			4.03			
5	PMS	27.38	4.68						
6			4.71	5.66	8.46				
7			4.69		8.23				
5	PRC	44.47	7.43						
6									
7									
5	BKR	53.36	8.88						
6			8.91	9.21					
7			9.88		10.58				
5	SBY	56.91	9.55	10.25					
6				10.30					
7									
5	BPZ	61.26	10.15	10.55	11.55				
6					11.63	11.98	12.98		
7			10.15		11.64				
5	PMR	71.33	12.25	13.04					23.55(S)
6									
7									
5	PWA	72.78		12.91					23.34(S)
6									
7				12.84					
5	SSN	77.00	12.51	13.34					
6									
7									
5	PME	77.06	12.65	13.92					24.62(S)
6									
7				14.02					
5	KNK	79.07		13.41					
6									
7			12.45		14.23				
5	RIZ	81.81	13.79	14.51					26.01(S)
6					15.07	15.69			
7			13.66		14.91				
5	MUR	85.55	13.70	14.35					
6						17.78	18.13	19.78	
7					16.00				
5	HTP	88.43	14.54	15.66					27.39(S)
6				15.67					
7			14.49	15.74					
5	SAW	114.02		19.12					
6									
7			18.02		19.62				
5	SKN	146.69		24.26					
6									
7									
5	SCM	154.63	25.17	25.77					
6									
7									

TABLE 4

	STA	D	\overline{TT}	$\langle TT \rangle$	RES
1	FTP	11.94	2.18	2.22	-.04
2	PMS	27.38	4.69	4.70	-.01
3	PRC	44.47	7.43	7.45	-.02
4	EXR	53.36	8.89	8.88	+.01
5	SBY	56.91	9.55	9.45	+.10
6	RPZ	61.26	10.15	10.15	0.00
7	PMR	71.33	12.25	11.77	+.48
8	PWA	72.78	(12.88)*	12.00	(+.88)*
9	SSN	77.00	12.51	12.68	-.17
10	PME	77.06	12.65	12.69	-.04
11	KNK	79.07	12.45	13.01	-.56
12	RIZ	81.81	13.73	13.45	+.28
13	MUR	85.55	13.70	14.05	-.35
14	HTP	88.43	14.52	14.52	0.00
15	SAW	114.02	18.02	18.63	-.61
16	SKN	146.69	24.26	23.88	+.38
17	SCM	154.63	25.17	25.16	+.01

*read as a direct (secondary) arrival and omitted from statistics

$$V_1 = 5.55 \quad V_2 = 6.22 \quad H_1 = 1.84 \quad N = 16$$

$$\text{Mean} = -0.03$$

$$\text{SDEV} = 0.29$$

$$+\text{EXT} = 0.48$$

$$-\text{EXT} = 0.61$$

$$\langle TT \rangle \equiv \frac{2\sqrt{D_1^2 + H_1^2}}{V_1} + \frac{D - 2D_1}{V_2}$$

$$\text{where } D_1 = H_1 \tan \theta_1$$

$$\text{and } \sin \theta_1 = \frac{V_1}{V_2}$$

$$\text{RES} \equiv \overline{TT} - \langle TT \rangle$$

\overline{TT} \equiv mean of the corrected travel times for first arrival.

Figure 1. Location map for seismic stations used to record the Bird Creek blasts. The solid triangles mark the locations of permanent stations, while the open triangles mark the locations of temporary stations established for the present study. Not shown on the map are the locations of other permanent stations (generally to the south of the blast site) nor those of the temporary stations established by the USGS along the roads south from the blast site to Seward.

Figure 2. Time-distance plot for the travel times of seismic waves from the Bird Creek blasts to the various recording stations. The corrected travel time is plotted against distance to the respective seismic station. The corrected travel time is the arrival time minus the origin time (of the blast) minus the elevation correction. The symbols are as follows: vertical bar = single arrival, triangle = double arrival or single first arrival, circle = triple arrival or double first arrival, square = triple first arrival. The data represented by solid symbols were used to calculate the slope and intercept of the line of the refracted arrivals. The data represented by open symbols were used to calculate the slope of the line of the direct arrivals; this line, by definition, is constrained to go through the origin.

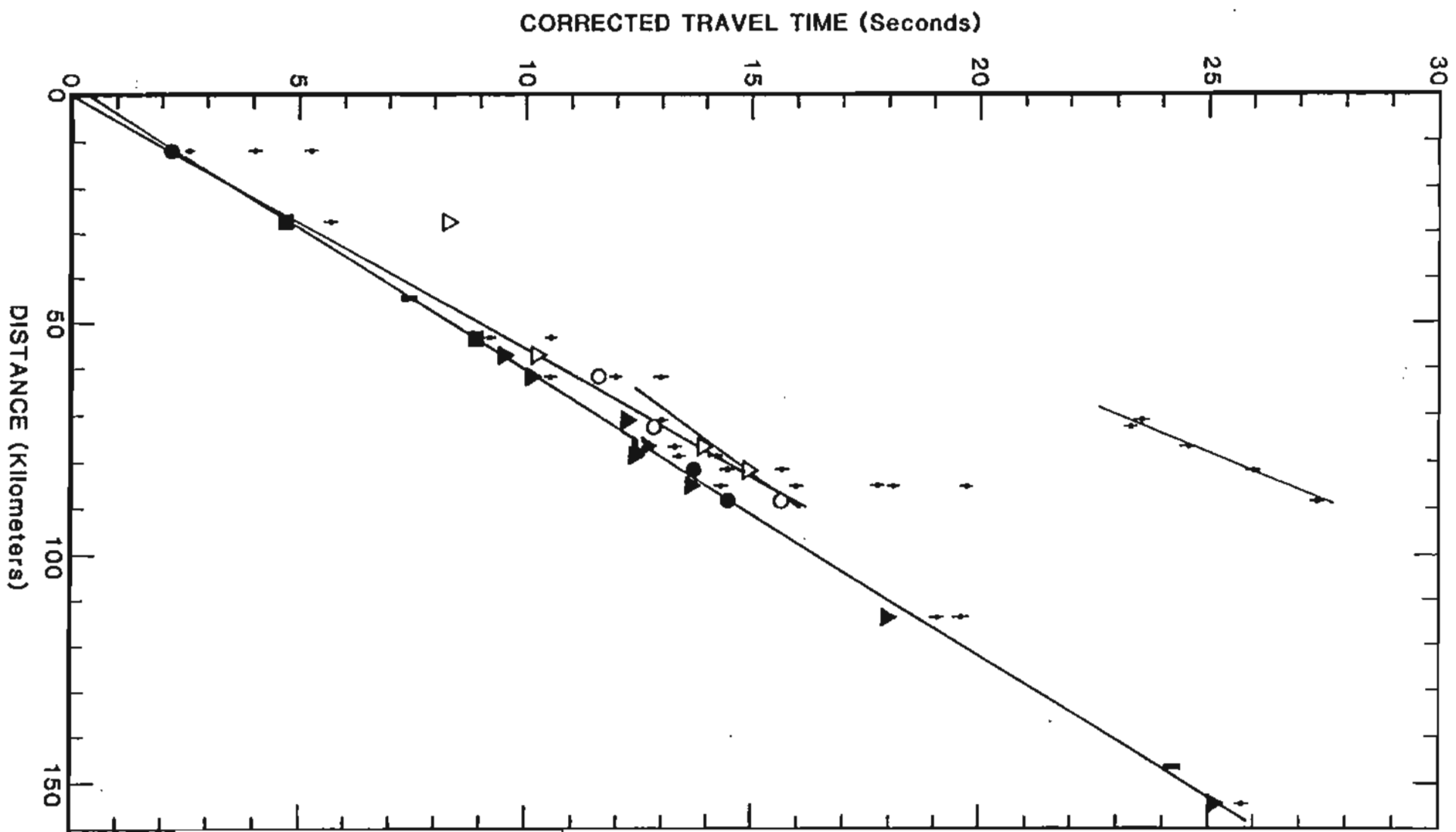


Figure 2